Fast Bo Insensitive Dixon Fat Suppression for Dynamic Breast MRI

T. Tashma Hoory[1], E. A. Ramsay[1], D. B. Plewes[1,2]

[1]Department of Imaging Research, Sunnybrook and Women's College Health Science Center, Toronto, Ontario, Canada, [2]Department of Medical Biophysics, University of Toronto, Toronto, Ontario, Canada

Project aim: We aim to demonstrate that a single-point "Dixon-like" water/fat separation method should be achievable for dynamic Gd-DTPA contrast enhanced imaging of the breast, if prior (pre-Gd) knowledge of the field-inhomogeneity phase shift and other phase shifts is used.

Introduction: After the Gd-DTPA bolus injection, data must be rapidly acquired over a limited (~ 10 minutes) period to track uptake kinetics for contrast enhanced breast MRI. Use of fat suppression pulses will substantially increase imaging time and will be sensitive to B_0 inhomogeneities. Two- or three-point Dixon variations[1] can overcome B_0 inhomogeneities but again require a substantial increase in imaging time. A 'single- point' method formerly proposed[2] sets the water and fat vectors at a relative angle of $\alpha \neq 2\pi n$. For a gradient echo, $\alpha = 2\pi\Delta f_{wf} TE$, where Δf_{wf} is the water/fat frequency shift. The signal in all voxels will follow the general form:

$$I = \left(W + \exp(i\alpha)\cdot F\right)\cdot \exp\left(-i\gamma\Delta B_0 \cdot TE - i\varphi_0\right) \qquad (1)$$

If the field inhomogeneity ΔB_0 and the spatially varying phase shifts φ_0 are known *a-priori*, one can proceed to find *W* and *F* directly in each voxel by computing:

$$\text{"dephasing" } I: \quad I' = I\cdot\exp\left(i\gamma\Delta B_0\cdot TE + i\varphi_0\right) \quad \Rightarrow \quad F = imag\left(I'\right)/\sin(\alpha) \;,\; W = real\left(I'\right) - \cos(\alpha)\cdot F \qquad (2)$$

Thereby obtaining a fast single-scan water/fat separation, with the added benefit of a freely chosen *TE*. Notice that if $\alpha=\pi/2$ one obtains the simple relations: *F=imag(I')* and *W=real(I')*. We propose to generate maps of ΔB_0 and φ_0 *before* the Gd injection and use these maps as a-priori data to *'dephase'* single-point images acquired *after* the injection. In this study, we test the idea in an oil-water breast phantom, using Gd-DTPA concentrations of the order of, and exceeding, those found in tumors during Gd-enhanced imaging of the breast.

Experimental Procedure: A GE 1.5T MRI scanner was used with a dedicated breast coil. The breast phantom (Figure 1) consists of a breast-shaped container filled with water and mineral oil. To simulate a tumor undergoing Gd-DTPA enhancement, a 25cc hollow sphere is incorporated into a flow circuit passing through the container. Gd-DTPA is added in monitored amounts to the water in the flow circuit and mixed by pump circulation. Initially, both the water in the phantom container and that filling the flow circuit are doped to the same level of 1mM Gd-DPTA to reduce relaxation times (obtainingT_1=210ms, T_2=175ms). ΔB_0 and φ_0 are mapped in the whole volume at this homogeneous doping stage, from a pair of FAST-SPGR 3d images acquired at the two in-phase *TE* values of 4.5 and 9ms. Next, the Gd-DTPA concentration of the water in the flow circuit is raised stepwise to levels of 1.5, 2, 3, and 4mM, resulting in [Gd] excesses of X = 0.5, 1, 2, and 3mM relative to the surrounding water in the breast phantom. At each Gd concentration, a single FAST-SPGR 3d imaging with *TE* = 3.4ms is carried out, corresponding to an angle of $\alpha=-\pi/2$ between water and fat. The previously derived distributions ΔB_0 and φ_0 are then used to 'dephase' all the single-point images, and the water and fat content of each voxel in each image is finally determined according to equation (2).

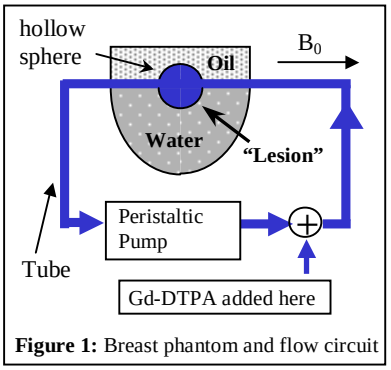

Figure 1: Breast phantom and flow circuit

Results: Fig. 2a,b shows the "water" and "fat" components obtained from the complex image at TE=3.4ms, when one simply assigns them to the real and (negative) imaginary parts of the complex image respectively, *without* correcting for ΔB_0 and φ_0. The data is that of the initial homogeneous 1mM doping stage. Substantial phase errors due to the uncorrected ΔB_0 and φ_0 phase factors obscure the water and fat distributions. However, when a-priori phase information is used to correct the complex images, as was done in Figures 2c-j, the water and fat distributions are recovered. In Fig 2c,d, the excess [Gd] in the ball+tube volume is zero and we note a good recovery of the fat/water components. The integrity of the water/fat separation is kept as the excess [Gd] increases to 0.5mM (figs 2e,f), and 1mM(figs 2g,h). An excess of 1mM is approximately twice the level found in breast cancers as determined by compartmental analysis, following an injected dose of 0.1mmole/kg [3]. At 3mM excess (figs 2i,j), the water/fat separation has clearly deteriorated. This results from an increasing change in ΔB_0 induced by the growing number of paramagnetic Gd ions, undermining the relevance of the a-priori ΔB_0 estimate.
To verify these results, the field ΔB_0 and phase φ_0 were *directly* mapped at the different doping excesses, X. We found a linear dependence throughout the image: $\Delta B_0(X) = AX + \Delta B_0(X=0)$, with *A* and $\Delta B_0(X=0)$ functions of the voxel coordinates. This agrees with the fact that a uniformly magnetized volume will always produce a field linear in the magnetization density. The values obtained for *A* outside the "tumor" are in agreement with those predicted by a direct calculation which takes into account the magnetic moment of the Gd ion and the geometric arrangement. Furthermore, the Gd-induced field outside the ball exhibits the expected dipole-like spatial pattern of a uniformly magnetized spherical shape (the tube volume being relatively small). In addition, φ_0 was left unchanged by the Gd, as expected.

Discussion: The extent of changes in ΔB_0 , and their spatial distribution, depend on the size and shape of the tumor phantom. In our phantom, the strongest Gd-induced field changes occurred within the narrow tube sections, and in regions adjacent to the ball. The simple geometric shapes of the straight tube and ball result in relatively simple field change patterns, which are probably more intense at some regions than would take place with realistic tumour geometry. For example, the narrow tube is characterized by a zero demagnetization factor, which leads to the tube volume possessing the strongest possible induced field. Thus, we expect the field changes induced by a realistic enhanced tumor not to peak as high (or as low) as those of our artificial configuration, and to be generally smoother.

Conclusions: The results indicate that ΔB_0 estimates preformed prior to Gd-DTPA injection remain relevant during the Gd-enhanced stage, for a wide range of Gd tissue concentrations of up to ~1mM. This is twice that expected in clinical breast applications. We conclude that fast, single point, fat/water separation can be used for dynamic breast MRI *without any increase in scan time* while successfully compensating for B_o field inhomgeneities.

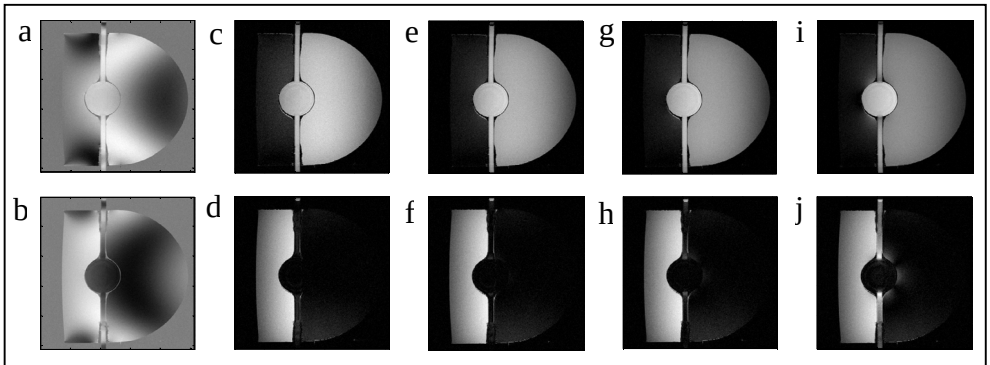

Figure 2: Fat (bottom row) and water images (top row). Images a,b obtained without any phase correction, while c-j use an a-priori (pre-Gd) phase correction. Excess Gd concentration in the ball+tubes increases from 0.0 (c,d) to 0.5 (e,f), 1.0 (g,h) and 3.0mM (i,j)

References:
[1] Glover GH, Schneider E, *Mag.Res.Med.* 18:371 (1991)
[2] Sepponen RE, Sipponen JT, Tanttu JI, *J Comput Assist Tomogr* 8:585 (1984) ; Paltiel Z, Ban A, *Proc.SMRM*, 4:172 (1985) ; Patrick JL, Haacke EM, Hahn JE *Proc.SMRM* 4:174(1985)
[3] Tofts PS, Berkowitz B, Schnall MD *Mag.Res.Med.*, 33:564 (1995)